ORIGINAL ARTICLE

Magnetic resonance imaging characterization of circumferential and longitudinal strain under various coronary interventions in swine

Mohammed SA Suhail, Mark W Wilson, Steven W Hetts, Maythem Saeed

Mohammed SA Suhail, Mark W Wilson, Steven W Hetts, Maythem Saeed, Department of Radiology and Biomedical Imaging, School of Medicine, University of California San Francisco, CA 94107-5705, United States

Mohammed SA Suhail, School of Medicine, University of California San Diego, CA 94107-5705, United States

Author contributions: Suhail MSA achieved and analyzed the images, prepared the figures and drafted the manuscript; Wilson MW and Hetts SW provided vital advices and were also involved in the editing; Saeed M designed the study, performed the experiments and wrote the final version of the manuscript.

Correspondence to: Maythem Saeed, PhD, Professor, Department of Radiology and Biomedical Imaging, School of Medicine, University of California San Francisco, 185 Berry Street, Suite 350, Campus Box 0946, San Francisco, CA 94107-5705, United States. msaeed@ucsf.edu

Telephone: +1-415-5146221 Fax: +1-415-3539423

Abstract

AIM: To compare the acute changes in circumferential and longitudinal strain after exposing a coronary artery to various interventions in swine.

METHODS: Percutaneous balloon angioplasty catheter was guided to location aid device (LAD) under X-ray fluoroscopy to create different patterns of ischemic insults. Pigs (*n* = 32) were equally divided into 4 groups: controls, 90 min LAD occlusion/reperfusion, LAD microembolization, and combined LAD occlusion/microembolization/reperfusion. Three days after interventions, cine, tagged and viability magnetic resonance imaging (MRI) were acquired to measure and compare left and right circumferential strain, longitudinal strain and myocardial viability, respectively. Measurements were obtained using HARP and semi-automated threshold method and statistically analyzed using unpaired *t*-test. Myocardial and vascular damage was characterized microscopically.

RESULTS: Coronary microemboli caused greater impairment in l left ventricular (LV) circumferential strain and dyssynchrony than LAD occlusion/reperfusion despite the significant difference in the extent of myocardial damage. Microemboli also caused significant decrease in peak systolic strain rate of remote myocardium and LV dyssynchrony. Cine MRI demonstrated the interaction between LV and right ventricular (RV) at 3 d after interventions. Compensatory increase in RV free wall longitudinal strain was seen in response to all interventions. Viability MRI, histochemical staining and microscopy revealed different patterns of myocardial damage and microvascular obstruction.

CONCLUSION: Cine MRI revealed subtle changes in LV strain caused by various ischemic insults. It also demonstrated the interaction between the right and left ventricles after coronary interventions. Coronary microemboli with and without acute myocardial infarction (AMI) cause complex myocardial injury and ventricular dysfunction that is not replicated in solely AMI.

Core tip: Cine and tagging magnetic resonance imaging showed that segments in pre-existing acute myocardial superimposed with microemboli have the most severe impairment in both longitudinal and circumferential strain, while segments subjected to solely microembolization or location aid device (LAD) occlusion/reperfusion showed only circumferential impairment. The

interaction between right and left ventricles after LAD interventions is clearly demonstrated by the increase in right ventricular (RV) free wall strain, suggesting that both left ventricular and RV need assessment in ischemic heart disease.

INTRODUCTION

Acute myocardial infarction (AMI) remains a leading cause of morbidity and mortality worldwide. It has been classified into subtypes based on clinical scenario; namely ischemia from a primary coronary event (*e.g.,* plaque rupture, thrombotic occlusion), ischemia from a supply-and-demand mismatch, and percutaneous/surgical coronary interventions[1]. Different procedures have been introduced to reperfused blocked major coronary artery. However, the effects of persistent microvascular blockage by dislodged microemboli are still a clinical problem, which has been acknowledged by multiple cardiac and interventional societies[2].

Echocardiography is the most commonly used clinical method for quantification of global and regional left ventricular (LV) function, where LV ejection fraction and wall motion score are measured[3]. Others used 2D speckle-tracking images for measuring regional strain and strain rate[4]. This method enables quantification of myocardial deformation[5], but associated with limitations, such as the inability of peak velocity to differentiate dyskinetic from hypokinetic myocardium[6]. Unlike other modalities, magnetic resonance imaging (MRI) provides quantitative prognostic functional and structural information[7,8]. Clinical MRI studies demonstrated the impairment in radial, circumferential and longitudinal strain in ischemic myocardium[9-11]. Investigators found that these MRI indices have higher sensitivity and specificity than 2D strain echocardiography in patients with AMI[12] and scar[13]. Furthermore, contrast enhanced MRI has the capability to delineate patchy myocardial infarct in patients[14] and animals[15-17]. However, the magnitude and mechanical effects of microemboli in pre-existing reperfused AMI on circumferential and longitudinal strain have not been characterized or compared to solely reperfused AMI using MRI. We hypothesized that coronary microemboli in pre-existing AMI cause complex ventricular dysfunction that is not replicated in solely AMI. Thus, this experimental investigation aimed at simulating 3 interventional clinical scenarios, namely location aid device (LAD) occlusion/reperfusion, LAD microembolization, and combined LAD occlusion/microembolization/reperfusion.

MATERIALS AND METHODS

Coronary intervention
This study was performed in accordance with the Guide for the Care and Use of Laboratory Animals and approval from IACUC. Farm pigs (30-32 kg) were sedated and anesthetized using isoflurane/oxygen 2%-5%/2-3 L/min. Small volume and size of microemboli (32 mm³ volume, average diameter 80 μm) were tested in the current study because previous autopsy study in humans showed that the sizes of these microemboli were less than 120 μm and most of microemboli (89%) were located in the LAD territory[18]. Accordingly, a 3F balloon catheter was advanced under X-ray fluoroscopy to the LAD coronary artery in swine model. The balloon catheter was used to (1) occlude (90 min) LAD coronary artery (*n* = 8), (2) delivery of microemboli (32 mm³ volume, about 120 microemboli with an average diameter of 80 μm (Embosphere®, Biosphere Med, Rockland, MA (*n* = 8), and (3) combine 90 min LAD occlusion and delivery of microemboli (32 mm³ volume, *n* = 8) followed by reperfusion. The occlusion or microemboli delivery was in the LAD at the middle of LV and the second diagonal branch was used as a land mark. Intravenous heparin and lidocaine were administered prior to coronary catheterization. ECG, heart rate, blood pressure, O2-sat, PCO2 and body temperature was monitored during the interventions. All animals were imaged 3 d after the interventions. Another 8 animals with matching body weight (30-32 kg) served as controls (no intervention).

Cardiac MRI
MRI was performed using 1.5-T scanner (GE Medical Systems, Milwaukee, WI, United States). For circumferential strain of the LV, a tagged turbo-field echo-planar sequence was used. The tagging technique used complementary spatial modulation of magnetization for horizontal and vertical tag orientation images obtained in one breath-hold. Imaging parameters were: TR/TE = 35/6.1 ms, flip = 25°, NEX = 1, section thickness = 8 mm, FOV = 24 cm × 24 cm, matrix = 128 × 45, pixel size = 1.875 × 5.333 mm², temporal resolution = 35 ms, EPI factor = 11, bandwidth = 185 Hz, echo length = 1, tag spacing = 5 mm, temporal resolution = 35 ms and cardiac phases = 16. Images were acquired in the short axis plane of the entire LV[19]. For quantitative analysis, two apical slices within the area of infarction (2.4 and 3.2 cm from the apex of the heart) were used. The tagging technique used complementary spatial modulation of magnetization for horizontal and vertical tag orientation images obtained in breath-hold and for longitudinal strain, multiple cine MR images in the long-axis view were acquired using a steady-state free precession sequence. Imaging parameters were: TR/TE/flip angle = 3.5 ms/1.75 ms/70°, slice thickness = 8 mm, no slice gap, FOV = 25 cm × 25 cm, matrix size = 160 × 152 and cardiac phases = 16.

For viability imaging, inversion-recovery gradient-echo DE-MRI images were acquired in the short and

long axis views of the heart. The imaging parameters were: TR/TE/flip angle = 5/2 ms/15°, interval = 2RR-intervals, slice thickness = 8 mm, no slice gap, FOV = 26 cm × 26 cm, matrix size = 256 × 162. Viability images were acquired 10-15 min after intravenous administration of 0.15 mmol/kg Gd-DTPA using inversion time of 220-230 ms to null remote myocardium. For quantitative measurement of large and patchy infarct a semi-automatic threshold method (3SD) was used. At the conclusion of the imaging sessions, the animals were sacrificed by intravenous injection of saturated KCl (1 mL/kg). The hearts were excised, sliced and incubated in 2% triphenyltetrazolium chloride (TTC) at 37 ℃. Digital images of TTC-stained slices were acquired, converted to black and white images using Adobe Photoshop CS2. The same semi-automatic method (3SD) used above was used to measure infarct size on TTC.

Image and statistical analysis

Phasic and peak longitudinal strain and circumferential strain were analyzed from complex raw data circumferential strain was obtained by manual outline of the endocardium and epicardium of the LV in multiple tagged images, which was automatically propagated by HARP tagged CMRI analysis software. The segmentation on HARP we done as follow: First, in a given timeframe, 2D HARP images were unwrapped in each slice[19]. Displacement measurements from the phase-unwrapped images were then used to compute a 3D displacement field from which strain was computed. This procedure was repeated for each imaged timeframe[20]. In each animal, two defined apical slices (2.4 and 3.2 cm from the apex of the heart) with infarct were analyzed. HARP software automatically provided strain at each point in the cardiac cycle, peak strain, time to peak strain (TTPS), and provided strain rate by obtaining a strain curve and differentiating the curve with respect to time[21]. Peak systolic and diastolic strain rate and TTP systolic and diastolic strain rates were obtained from these curves.

Peak systolic longitudinal strain was obtained from a 4 chamber view of cine MR images after delineating endocardial length of LV and right ventricular (RV) during systole and diastole using an echocardiographic method[22,23]. Figure 1 shows the semi-automated traced myocardium throughout the cardiac cycle. Longitudinal strain was determined in LV free wall (LVFW), RV free wall (RVFW), and interventricular septum (IVS). This method has been recently validated against spatial modulation of magnetization tissue tagging method[24]. Semi-automatic threshold method (+3SD), ImageJ was also used to measure large infarct and patchy microinfarct on contrast enhanced MRI and histochemical TTC staining. Paired and unpaired nonparametric Student *t*-tests and nonparametric ANOVA with Dunn's multiple comparison tests were used. A $P < 0.05$ was considered significant.

Postmortem staining

At the conclusion of the imaging protocol, the hearts were excised, sliced and incubated in 2% TTC at 37 ℃

for 30 min. Digital images of TTC stained short-axis slices were acquired and converted to black-and-white images. For confirmation of structural changes caused by coronary interventions, 3 LV rings from each animal were fixed in 10% buffered formalin, processed, sectioned and stained with hematoxylin/eosin. Microscopically, the stained sections were magnified (× 40 to × 100), photographed under light microscopy using NIS Elements-F (Nikon, Melville, NY, United States) and studied.

RESULTS

Myocardial viability

Control animals revealed no evidence of infarction on DE-MRI and TTC staining or differential strain between LAD territory and remote myocardium (Figure 2A, $P = 0.72$). The different interventions produced continuous, patchy or combined pattern of enhancement of myocardial damage on DE-MRI. Furthermore, myocardial damage was significantly smaller (8.8% ± 0.5% LV mass) in solely microembolized animals compared with animals subjected to occlusion/reperfusion (12.4% ± 1.2%, $P < 0.01$) or the combination of the two insults (15.7% ± 1.1%, $P < 0.05$).

Circumferential strain

All animals subjected to coronary interventions demonstrated decline in peak circumferential strain compared with remote myocardium (Figure 2A, all $P < 0.001$) or LAD territory of control animals (Figure 2B). However, peak circumferential strain showed no difference between interventions, suggesting disproportion between myocardial damage and regional strain. At 3 d, remote myocardium of animals subjected to interventions showed decreased TTPS without increase in circumferential strain compared with controls (Figure 2B). In contrast, the LAD territory demonstrated increased TTPS (Figure 2C), suggesting LV dyssynchrony.

All interventions caused significant decrease in peak strain rate of LAD territory compared with remote myocardium and controls (Figure 3A and B, all $P < 0.001$). Microembolized and combined intervention animals had significantly decreased systolic strain rate compared to LAD occluded/reperfused animals. In remote myocardium, peak systolic strain rate was significantly decreased in microembolized and combined insult animals, but not in occluded/reperfused animals, compared with controls. Additionally, all interventions caused decreased peak diastolic strain rate in the LAD territory compared with controls (Figure 3C). Similar to peak systolic strain rate, peak diastolic strain rate in remote myocardium was significantly decreased in animals subjected to microembolization or combined interventions, but not in LAD occluded/reperfused animals, compared with controls. Remote myocardium also showed significantly decreased TTP systolic and diastolic circumferential strain rates in animals subjected to microembolization or combined intervention (Figure 4), but not in LAD occluded/reperfused animals.
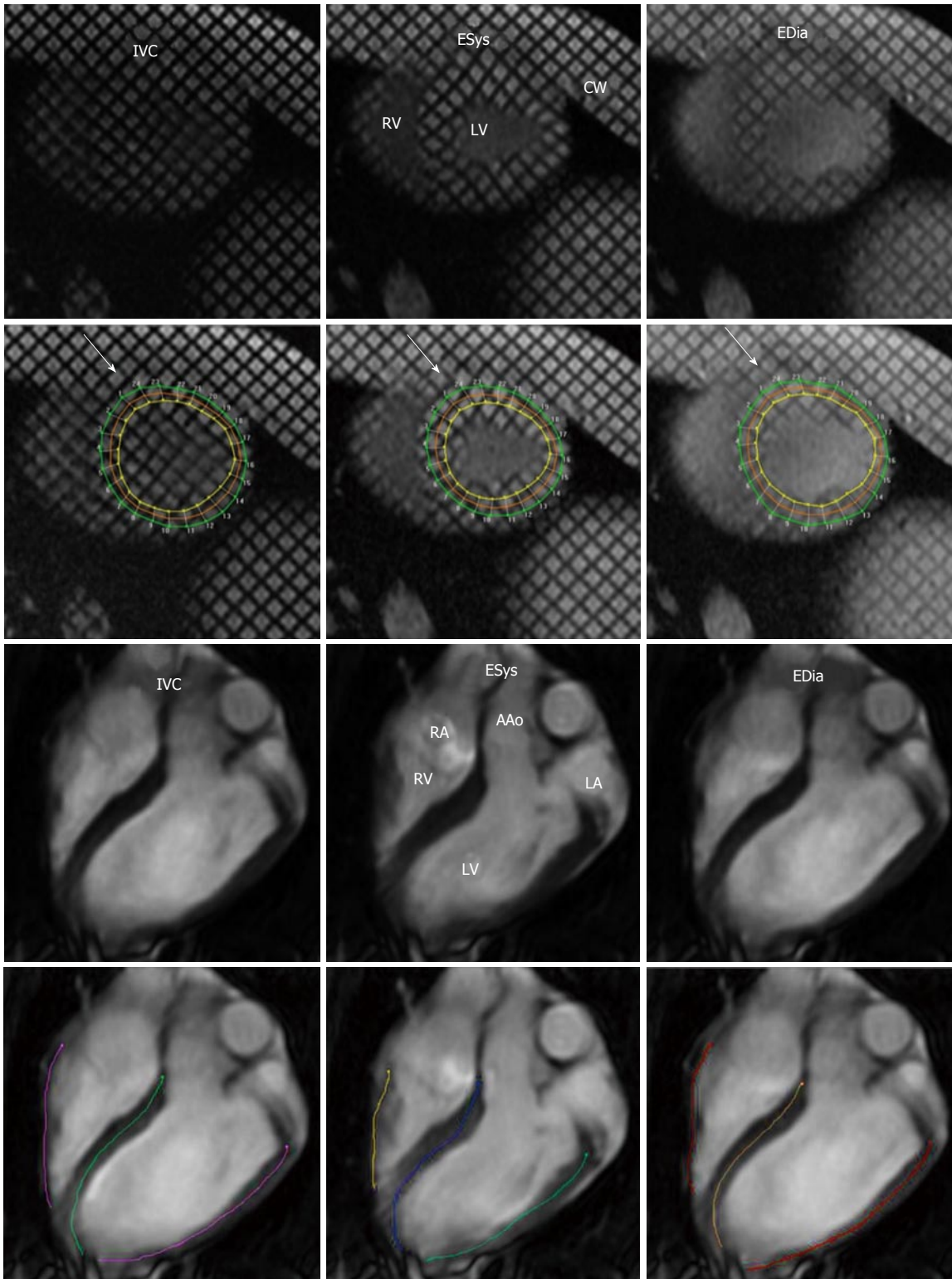
Figure 1 Representative tagged and cine magnetic resonance images with tracing method. Top row demonstrates short-axis and long-axis magnetic resonance images (MRI) images, while bottom row demonstrates images after tracing of the myocardium using HARP. Left three columns are cine tagged MRI and right three columns are cine MRI. IVC: Isovolumetric contraction; ESys: End systole; EDia: End diastole; LV: Left ventricle; RV: Right ventricle; CW: Chest wall; RA: Right atrium; LA: Left atrium; AAo: Ascending aorta.

Longitudinal strain

Figure 5 demonstrates strain curves during the cardiac cycle for each cohort. No significant change in longitudinal strain was observed in both LVFW and IVS of animals 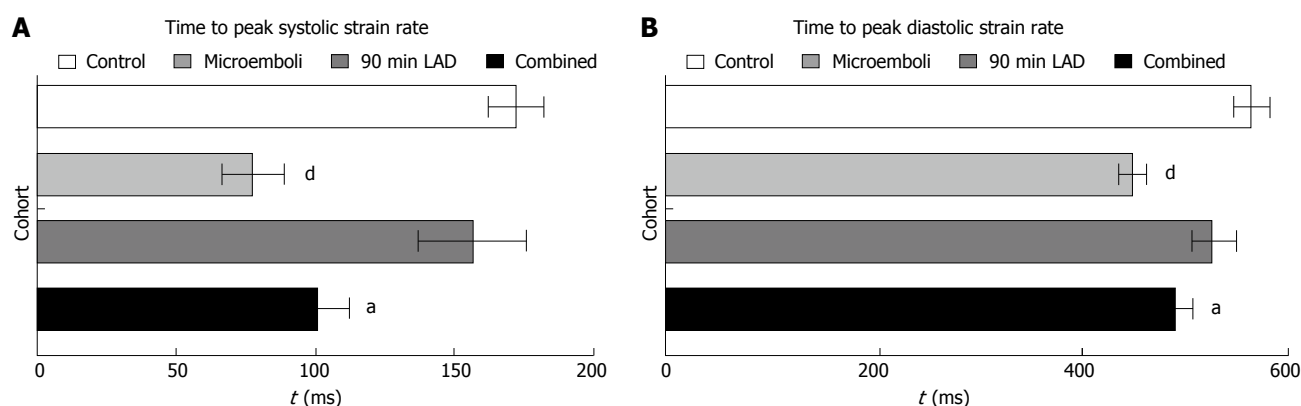subjected microembolization or LAD occlu-sion/reperfusion compared with controls (Figure 5). In contrast, animals subjected LAD occlusion/microembo-lization/reperfusion showed significant compensatory increased peak longitudinal strain in the RVFW. Unlike other groups, animals subjected to LAD occlusion/mi-
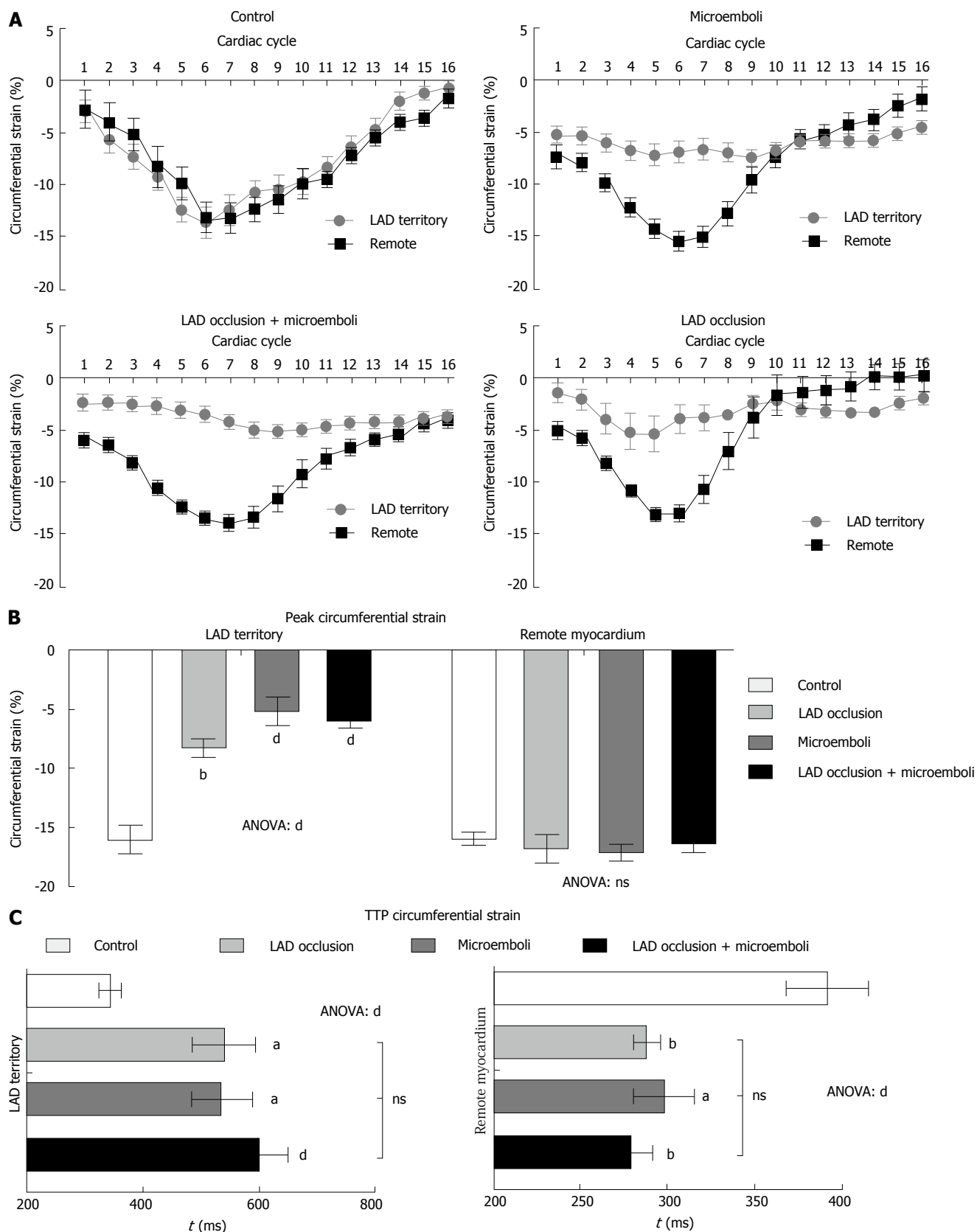
Figure 2 Circumferential strain analysis: phasic, peak, and territory time to peak strain. A: Phasic circumferential strain peak and rate during one R-R interval in LAD territory and remote myocardium of the 4 groups. Data are presented as means ± SEM. A significantly decreased peak circumferential strain was observed in the LAD territory compared with remote myocardium in all coronary interventions ($P < 0.001$); B: Bars show average peak circumferential strain. ANOVA showed significant decrease in strain of the LAD territory 3 d after interventions compared with controls. Remote myocardium showed no significant difference between interventions and control; C: shows significant variation in time to peak circumferential strain between remote and the LAD territory time to peak strain (TTPS). Remote myocardium showed decreased TTPS for all interventions, while the LAD territory demonstrated increased TTPS. Control *vs* LAD, [a]$P < 0.05$; Control *vs* Microemboli, [b]$P < 0.01$; Control *vs* ANOVA [d]$P < 0.001$. LAD: Location aid device.
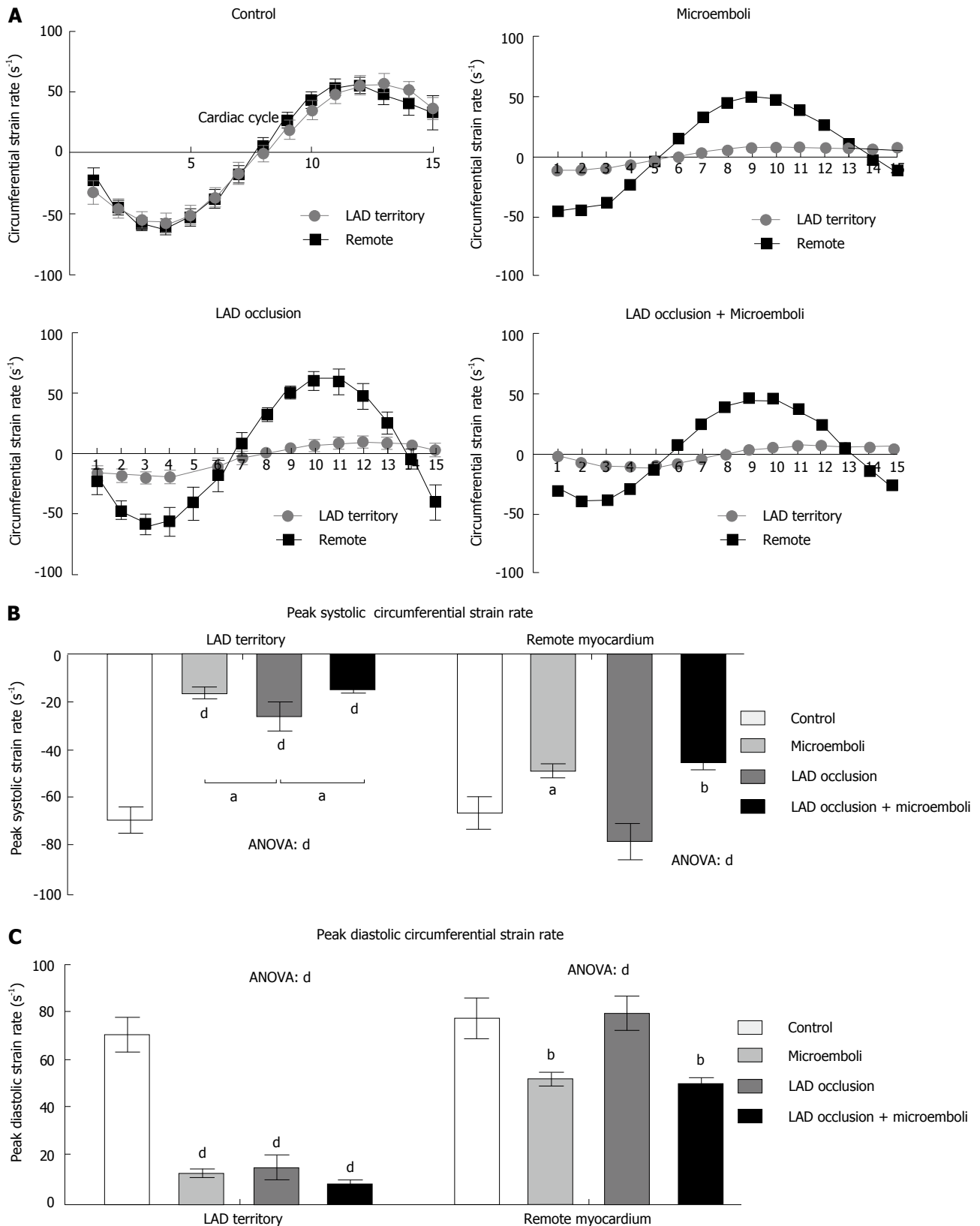
Figure 3 Circumferential strain rate analysis: phasic, peak, and territory time to peak systolic and diastolic strain rate. A: Circumferential strain rate curves. Data are presented as means ± SEM. In control animals, remote myocardium and location aid device (LAD) territory have identical curves, while remote *vs* LAD territory in all interventions were significantly different (*P* < 0.001); B: The LAD territory showed significantly decreased systolic strain rate in LAD territory for all interventions, with microembolized and combined groups significantly less than solely LAD occlusion. Remote myocardium showed only a decrease in microembolized and combined groups; C: The LAD territory demonstrated significantly decreased diastolic strain rate in LAD territory for all interventions. Remote myocardium again showed only significant decrease in microembolized and combined groups. Control *vs* LAD, [a]*P* < 0.05; Control *vs* Microemboli, [b]*P* < 0.01; Control *vs* ANOVA [d]*P* < 0.001.

A Time to peak systolic strain rate

☐ Control ▨ Microemboli ▨ 90 min LAD ■ Combined

B Time to peak diastolic strain rate

☐ Control ▨ Microemboli ▨ 90 min LAD ■ Combined

Figure 4 Time to peak systolic and diastolic strain rate in remote myocardium. Remote myocardium peak systolic (left) and diastolic strain rate (right) in controls and animals subjected to interventions. Only animals subjected to microembolization or combined ischemic insults showed significantly earlier systolic and diastolic strain rates. Data are presented as means ± SEM. Control *vs* Combined, $^{a}P < 0.05$; Control *vs* Microemboli, $^{d}P < 0.001$. LAD: Location aid device.

croembolization/reperfusion showed severe reduction in IVS longitudinal strain compared with controls (Figure 5).

Microscopic examination

Microscopic examinations revealed both patchy and homogeneous myocardial damage (depending on the type of the insult), microvascular damage and obstruction in all animals subjected to coronary interventions, but not controls. The microemboli were settled either individually or in clusters in the intravascular compartment (Figure 6). LAD occlusion/reperfusion animals showed contiguous myocardial damage associated with severe interstitial edema, intramyocardial hemorrhage and inflammation, while animals subjected to LAD occlusion/microembolization/reperfusion showed contiguous infarct containing severe intramyocardial hemorrhage, edema, deposited calcium in the core and patchy microinfarct at the border zone.

DISCUSSION

The major findings of this study are that (1) there was disproportion between the decline in circumferential strain, dyssynchrony and myocardial damage of animals subjected to microembolization and LAD occlusion/reperfusion; (2) microemboli caused unique effect on remote myocardial strain rates not seen in LAD occlusion/reperfusion group; (3) unlike LAD occlusion/reperfusion group, microemboli produced persistent microvascular obstruction, which may explain the difference in strain and dyssynchrony between the groups; and (4) MRI demonstrated the interaction between LV and RV, where compensatory longitudinal strain increase in the RVFW was evident in all coronary interventions.

Microvascular obstruction

Clinical studies have demonstrated that patients with CMR-defined microvascular obstruction have significantly increase cardiovascular events in follow up[25]. Galiuto[26] has recently classified microvascular damage to structural (irreversible) or functional (reversible), where

the structural damage is related damage of microvascular walls; conversely, the functional damage is related to edema and cellular plugging. This MR study focused on the effects of persistent MVO caused by LAD microembolization, with and without pre-existing AMI and compared it with reperfused infarct (reperfusion injury). Our histologic examination revealed that the microvascular are patent, but modeled, in LAD occlusion/reperfusion group, but persistently obstructed in microembolized groups. Funaro *et al*[27] indicated that coronary microvascular obstruction is the strongest predictor of post-ischemic myocardial dysfunction and strongly associated with increased morbidity and mortality.

Circumferential strain

The contraction pattern is an important measure of LV function and independent of EF, wall motion abnormalities or MVO₂[19]. Early methods for measuring LV strain had limitations in resolution and subjectivity[28]. Echocardiography showed that visual tracking is insufficient to assess strain[29] and peak velocity cannot differentiate dyskinetic from hypokinetic myocardium[6]. Other used Doppler-based imaging or speckle tracking for strain and dyssynchrony measurement, but this approach has other limitation, such as 2D, intersegmental tethering, cardiac motion, dependence of measurements upon the angle and low image quality[6,29,30].

Recent studies showed that the complex contraction pattern of the heart and alterations to this pattern due to various cardiac pathologies could be determined using tagged cine MRI[9-11]. Therefore, tagged cine MRI has been used in patients with corrected Tetralogy of Fallot and near-normal EF. Investigators found decreased circumferential strain in the basal and apical LV slices and dyssynchronous basal rotation[11]. While previous occlusion/reperfusion studies have shown correlation between infarct size and measurements of contraction pattern (such as circumferential strain and TTPS)[12,13]. This MR study demonstrated that peak strain and TTPS are early predictors of dysfunction. Surprisingly, 4/8 animals at 3 d with transmural infarcts on contrast enhanced MRI
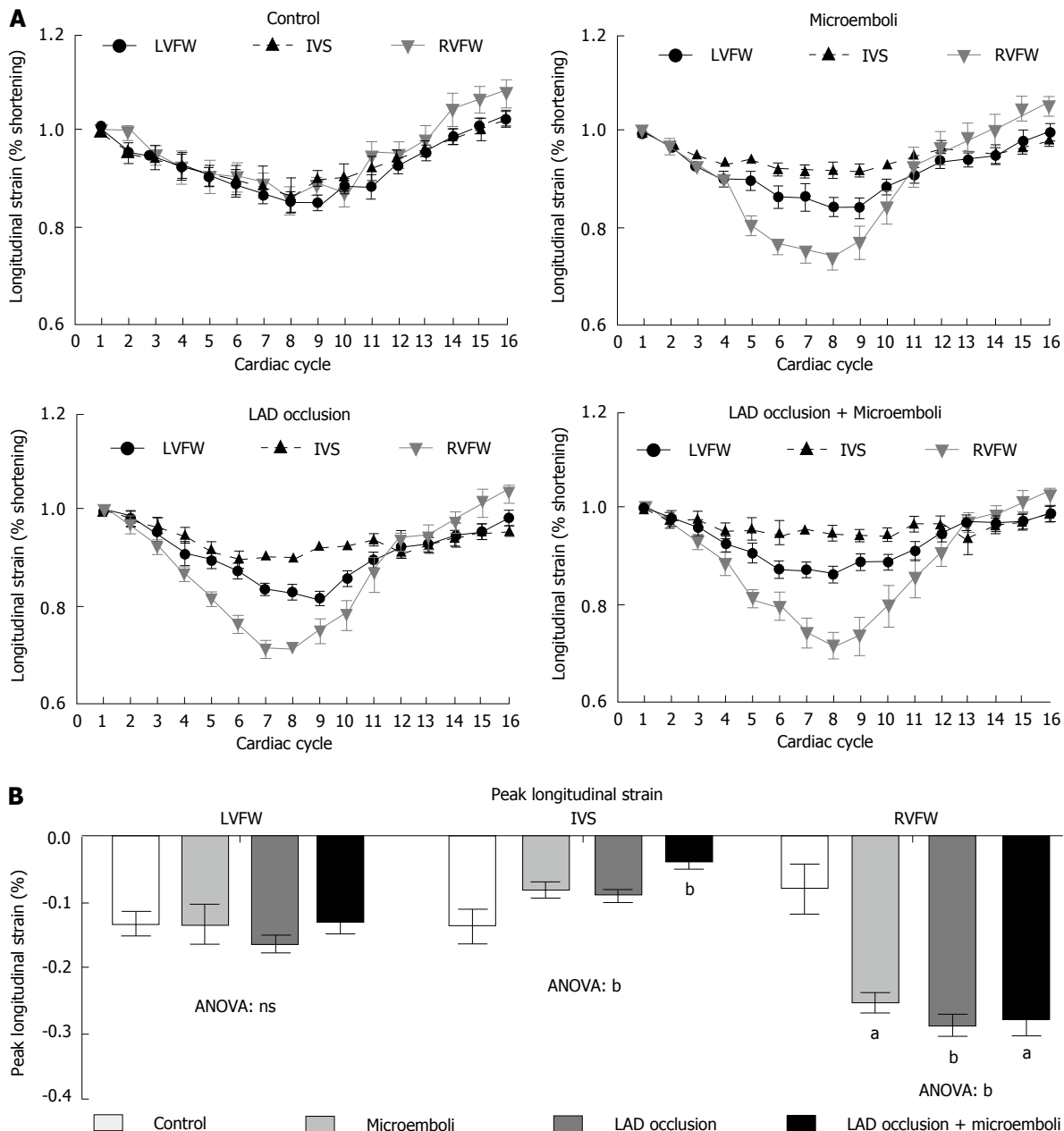
Figure 5 Longitudinal strain analysis: phasic and peak. A: Phasic longitudinal strain rate curves quantitatively show increased strain in right ventricular free wall (RVFW) and decreased strain in interventricular septum (IVS); B: Peak longitudinal strain. All interventions showed compensatory increase in peak strain in RVFW, while significantly decreased longitudinal peak strain was only seen in the IVS of combined insult animals. Data are presented as means ± SEM. Control *vs* Microemboli, [a]*P* < 0.05; Control *vs* LAD Occlusion, [b]*P* < 0.01. LAD: Location aid device; LVFW: Left ventricular free wall.

demonstrated circumferential strain, confirming previous findings that systolic and diastolic strain of an infarcted segment is complex interaction[31].

Investigators have found that interventricular dyssynchrony is another measure of prognosis[32]. Our data showed LV dyssynchrony in all interventions, as evidenced by increased TTPS in LAD territory and decreased TTPS in remote myocardium. It has been shown that patients with dyssynchrony are much more likely to develop LV remodeling than those without dyssynchrony (91% *vs* 2%)[33], because the pathophysiological remodeling process likely begins with a disorganized pattern of contraction[34]. In the current study, all interventions caused significant dyssynchrony and underscored the disproportion of infarct size to functional myocardial damage. We also found unique strain rate changes in remote myocardium related to microembolization only. These measurements may yield valuable information on the pathogenesis of ischemic cardiomyopathy, which seems to have similar remodeling and is still poorly understood[30].

Longitudinal strain

It has been shown that RV has greater longitudinal pumping component than the LV[8]. Our study showed that all coronary interventions caused significant increase in peak systolic longitudinal strain of the RVFW. The changes
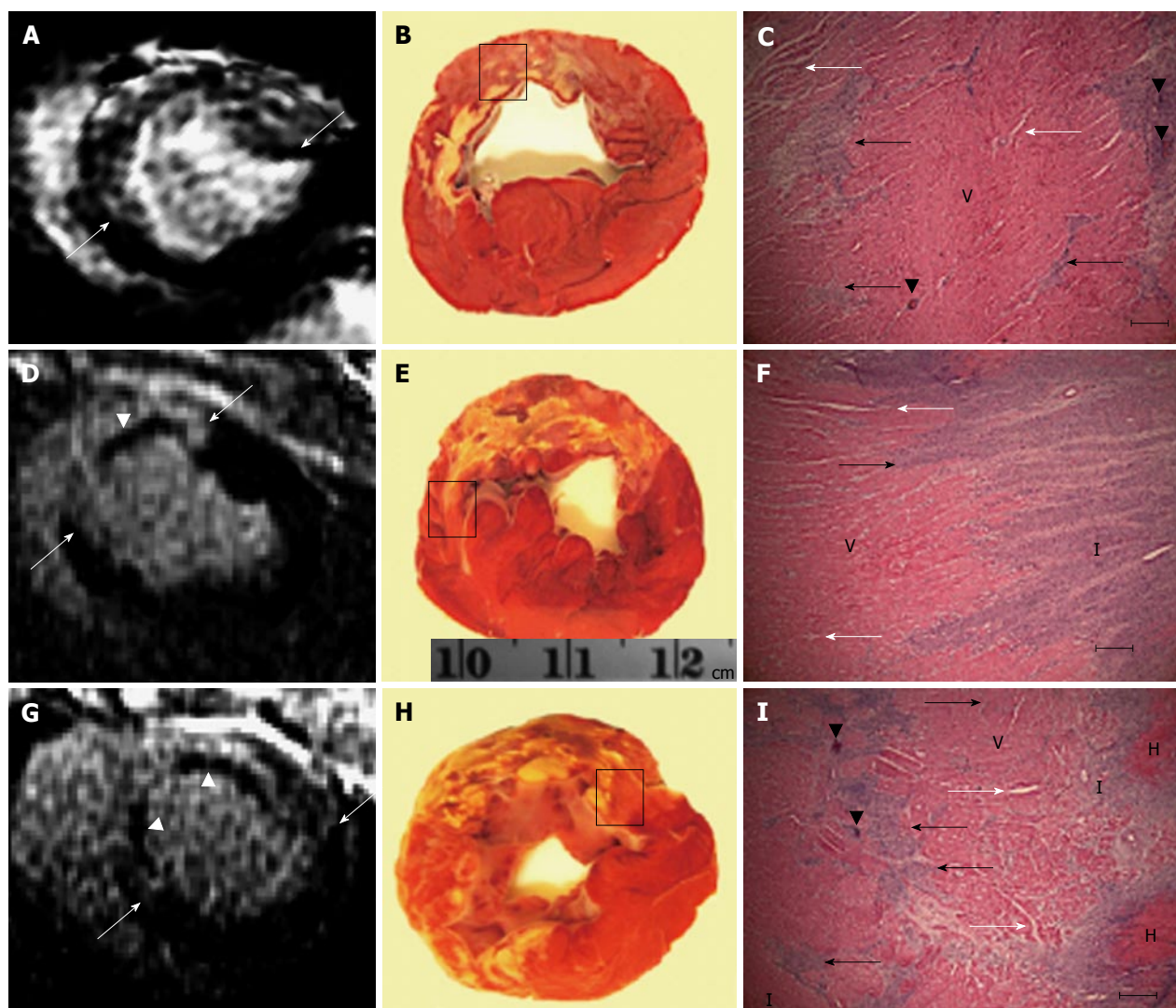
Figure 6 Viability contrast enhanced magnetic resonance images postmortem histochemical triphenyltetrazolium chloride stain and microscopy in animals subjected to soley microinfarction (top), soley location aid device occlusion/reperfusion (middle) and combined location aid device occlusion/reperfusion and microembolization (bottom). A: MR image and TTC stain show patchy microinfarct in the LAD territory; B: Postmortem histochemical TTC stain; C: Shows necrotic small islands (black arrows), interstitial edema (white arrow) and microemboli (black arrowhead); D: MR image shows the large infarct (white arrows) with hypoenhanced microvascular obstruction zone (white arrowhead); E: TTC section shows transmural infarct; F: Microinfarct tethering (black arrows) and interstial edema (white arrows) at the edge of the infarct; G: MR image shows the large infarct with patchy hyperenhanced microinfarct in the peri-infarct region (white arrows) with very large hypoenhanced microvascular obstruction zones (white arrowhead); H: TTC section shows hemorrhagic transmural infarct with patchy microinfarct in the peri-infarct region; I: Necrotic small islands (black arrows), interstitial edema (white arrow) and microemboli (black arrowhead). V: Viable myocardium, H: Hemorrhage; I: Large infarct. TTC: Triphenyltetrazolium chloride; MRI: Magnetic resonance imaging; LAD: Location aid device.

in the RVFW function after LV insult clearly indicate interventricular interaction and stressing the importance of evaluating both ventricles in cases of myocardial infarction. Previous studies have shown that longitudinal strain correlates to infarct size[35], Combined intervention impaired longitudinal strain in IVS that is not detectable in LAD occlusion/reperfusion group. It should be noted that our method for measuring peak systolic longitudinal strain is easy and quick enough to be applied in clinical practice. Furthermore, the acquired steady state free precession cine MR images can be used without the need to perform additional tagging imaging and it has been recently validated against spatial modulation of magnetization tissue tagging method[24]. We propose that the improvement in strain is an index of myocardial viability and is associated with global LV l improvement and may reverse remodeling, which is an important predictor of a favorable long-term outcome[26].

Study limitations

The synthetic microemboli used in this study may exhibit no inflammatory reaction, but previous enzymatic assay[36] and microscopy[16] demonstrated inflammatory reactions. Another limitation is that the longitudinal strain rate was not measured manually. A semi-automatic feature-tracking software has been recently used for assessing strain rate (TomTec Imaging Systems, Munich, Germany)[24].

In conclusion, this MRI study suggests that circum-

ferential and longitudinal strain and strain rate are sensitive and noninvasive indices of ventricular dysfunction. Patchy microinfarction is a complex ischemic injury, which features disproportionate functional impairment in the LV, including unique and dominant effects on global LV function that is not replicated by LAD occlusion/reperfusion, which represents "classic" acute MI. All interventions showed dynamic interaction between left and right ventricles. Furthermore, MRI has the potential to grade the severity of myocardial injury in various ischemic insults and identifies left and right ventricular dysfunction associated with myocardial damage.

ACKNOWLEDGMENTS

COMMENTS

Background
The use of percutaneous coronary intervention (PCI) has been a mainstay of treatment in acute myocardial infarctions in the past few decades. While these interventions are life-saving, they have been recently found to cause their own kinds of long term damage to the heart. Breaking of large clots into smaller ones causes these smaller microemboli to lodge in small blood vessels and damage the heart. Cardiac magnetic resonance imaging (MRI) is being used more frequently to study cardiac morphology and function, which was previously ascertained with less exact and operator-dependent methods, such as echocardiography. Cardiac MRI is thus an excellent imaging modality to assess damage after PCI.

Research frontiers
Research into the insidious effects of PCI has been improved with the use of cardiac MRI. While cardiac MRI has historically been used mostly in the imaging and follow up of congenital heart diseases, it is more frequently being used in routine clinical care and in the research settings of cardiac pathology that was once difficult to image precisely.

Innovations and breakthroughs
This article suggests that the effects of microemboli from PCI may be causing unique damage that has not previously been reported. Certain measurements of strain and strain rate, which are available only from cardiac MRI, demonstrated changes in the group of animals that had microemboli but not in those that simply had an occluded coronary without treatment. This suggests that the effects of PCI need to be more adequately studied. This paper also demonstrated and further validated a PCI model in swine.

Applications
This research should be taken into the context of the massive amount of literature in regards to percutaneous coronary intervention. While PCI may have risks, it is often a life-saving procedure and clinical practice should not change based on the results of this research. However, more research into the effects of PCI, especially the long term effects of microemboli, should be undertaken in order to adequately assess PCI risk and help to improve the procedure itself to prevent or alleviate these sequelae.

Terminology
Percutaneous coronary intervention: an intervention done by a cardiologist during AMIs, or "heart attacks" to relieve a blockage, usually from a clot, in the arteries that feed the heart. The most important of these arteries is the Left Anterior Descending artery, or location aid device. MRI is a form of imaging that utilizes a large magnet and radiofrequency pulses which does not cause any harmful radiation.

Peer review
This is a good study of the effects of microembolization from PCI on the cardiac function of swine. The results are interesting and suggest that PCI may have harmful effects that were not previously known. The long term changes in these effects needs to be further researched.

REFERENCES

1   **Thygesen K**, Alpert JS, White HD. Universal definition of myocardial infarction. *Eur Heart J* 2007; **28**: 2525-2538 [PMID: 17951287 DOI: 10.1093/eurheartj/ehm355]

2   **Anderson JL**, Adams CD, Antman EM, Bridges CR, Califf RM, Casey DE Jr, Chavey WE 2nd, Fesmire FM, Hochman JS, Levin TN, Lincoff AM, Peterson ED, Theroux P, Wenger NK, Wright RS, Smith SC Jr, Jacobs AK, Adams CD, Anderson JL, Antman EM, Halperin JL, Hunt SA, Krumholz HM, Kushner FG, Lytle BW, Nishimura R, Ornato JP, Page RL, Riegel B; American College of Cardiology; American Heart Association Task Force on Practice Guidelines (Writing Committee to Revise the 2002 Guidelines for the Management of Patients With Unstable Angina/Non-ST-Elevation Myocardial Infarction); American College of Emergency Physicians; Society for Cardiovascular Angiography and Interventions; Society of Thoracic Surgeons; American Association of Cardiovascular and Pulmonary Rehabilitation; Society for Academic Emergency Medicine. ACC/AHA 2007 guidelines for the management of patients with unstable angina/non-ST-Elevation myocardial infarction: a report of the American College of Cardiology/American Heart Association Task Force on Practice Guidelines (Writing Committee to Revise the 2002 Guidelines for the Management of Patients With Unstable Angina/Non-ST-Elevation Myocardial Infarction) developed in collaboration with the American College of Emergency Physicians, the Society for Cardiovascular Angiography and Interventions, and the Society of Thoracic Surgeons endorsed by the American Association of Cardiovascular and Pulmonary Rehabilitation and the Society for Academic Emergency Medicine. *J Am Coll Cardiol* 2007; **50**: e1-e157 [PMID: 17692738 DOI: 10.1016/j.jacc.2007.02.013]

3   **Lang RM**, Bierig M, Devereux RB, Flachskampf FA, Foster E, Pellikka PA, Picard MH, Roman MJ, Seward J, Shanewise JS, Solomon SD, Spencer KT, Sutton MS, Stewart WJ. Recommendations for chamber quantification: a report from the American Society of Echocardiography's Guidelines and Standards Committee and the Chamber Quantification Writing Group, developed in conjunction with the European Association of Echocardiography, a branch of the European Society of Cardiology. *J Am Soc Echocardiogr* 2005; **18**: 1440-1463 [PMID: 16376782 DOI: 10.1016/j.echo.2005.10.005]

4   **Møller JE**, Hillis GS, Oh JK, Reeder GS, Gersh BJ, Pellikka PA. Wall motion score index and ejection fraction for risk stratification after acute myocardial infarction. *Am Heart J* 2006; **151**: 419-425 [PMID: 16442909 DOI: 10.1016/j.ahj.2005.03.042]

5   **Reisner SA**, Lysyansky P, Agmon Y, Mutlak D, Lessick J, Friedman Z. Global longitudinal strain: a novel index of left ventricular systolic function. *J Am Soc Echocardiogr* 2004; **17**: 630-633 [PMID: 15163933 DOI: 10.1016/j.echo.2004.02.011]

6   **Thibault H**, Derumeaux G. Assessment of myocardial ischemia and viability using tissue Doppler and deformation imaging: the lessons from the experimental studies. *Arch Cardiovasc Dis* 2008; **101**: 61-68 [PMID: 18391875 DOI: 10.1016/S1875-2136(08)70257-2]

7   **Dicks DL**, Carlsson M, Heiberg E, Martin A, Saloner D, Arheden H, Saeed M. Persistent decline in longitudinal and radial strain after coronary microembolization detected on velocity encoded phase contrast magnetic resonance imaging. *J Magn Reson Imaging* 2009; **30**: 69-76 [PMID: 19557848 DOI: 10.1002/jmri.21773]

8   **Carlsson M**, Osman NF, Ursell PC, Martin AJ, Saeed M. Quantitative MR measurements of regional and global left ventricular function and strain after intramyocardial transfer of VM202 into infarcted swine myocardium. *Am J Physiol Heart Circ Physiol* 2008; **295**: H522-H532 [PMID: 18539758

DOI: 10.1152/ajpheart.00280.2008]

9   **Croisille P**, Moore CC, Judd RM, Lima JA, Arai M, McVeigh ER, Becker LC, Zerhouni EA. Differentiation of viable and nonviable myocardium by the use of three-dimensional tagged MRI in 2-day-old reperfused canine infarcts. *Circulation* 1999; **99**: 284-291 [PMID: 9892596 DOI: 10.1161/01. CIR.99.2.284]

10 **Götte MJ**, van Rossum AC, Twisk JWR JT, Visser CA. Quantification of regional contractile function after infarction: strain analysis superior to wall thickening analysis in discriminating infarct from remote myocardium. *J Am Coll Cardiol* 2001; **37**: 808-817 [PMID: 11693756 DOI: 10.1016/S0735-1097(00)01186-4]

11 **Marcus JT**, Götte MJ, Van Rossum AC, Kuijer JP, Heethaar RM, Axel L, Visser CA. Myocardial function in infarcted and remote regions early after infarction in man: assessment by magnetic resonance tagging and strain analysis. *Magn Reson Med* 1997; **38**: 803-810 [PMID: 9358455 DOI: 10.1002/mrm.1910380517]

12 **Migrino RQ**, Zhu X, Pajewski N, Brahmbhatt T, Hoffmann R, Zhao M. Assessment of segmental myocardial viability using regional 2-dimensional strain echocardiography. *J Am Soc Echocardiogr* 2007; **20**: 342-351 [PMID: 17400112 DOI: 10.1016/j.echo.2006.09.011]

13 **Rosendahl L**, Blomstrand P, Brudin L, Tödt T, Engvall JE. Longitudinal peak strain detects a smaller risk area than visual assessment of wall motion in acute myocardial infarction. *Cardiovasc Ultrasound* 2010; **8**: 2 [PMID: 20064264 DOI: 10.1186/1476-7120-8-2]

14 **Choi JW**, Gibson CM, Murphy SA, Davidson CJ, Kim RJ, Ricciardi MJ. Myonecrosis following stent placement: association between impaired TIMI myocardial perfusion grade and MRI visualization of microinfarction. *Catheter Cardiovasc Interv* 2004; **61**: 472-476 [PMID: 15065140 DOI: 10.1002/ccd.20024]

15 **Breuckmann F**, Nassenstein K, Bucher C, Konietzka I, Kaiser G, Konorza T, Naber C, Skyschally A, Gres P, Heusch G, Erbel R, Barkhausen J. Systematic analysis of functional and structural changes after coronary microembolization: a cardiac magnetic resonance imaging study. *JACC Cardiovasc Imaging* 2009; **2**: 121-130 [PMID: 19356544 DOI: 10.1016/j.jcmg.2008.10.011]

16 **Saeed M**, Hetts SW, Ursell PC, Do L, Kolli KP, Wilson MW. Evaluation of the acute effects of distal coronary microembolization using multidetector computed tomography and magnetic resonance imaging. *Magn Reson Med* 2012; **67**: 1747-1757 [PMID: 21956356 DOI: 10.1002/mrm.23149]

17 **Carlsson M**, Saloner D, Martin AJ, Ursell PC, Saeed M. Heterogeneous microinfarcts caused by coronary microemboli: evaluation with multidetector CT and MR imaging in a swine model. *Radiology* 2010; **254**: 718-728 [PMID: 20177087 DOI: 10.1148/radiol.09090527]

18 **Schwartz RS**, Burke A, Farb A, Kaye D, Lesser JR, Henry TD, Virmani R. Microemboli and microvascular obstruction in acute coronary thrombosis and sudden coronary death: relation to epicardial plaque histopathology. *J Am Coll Cardiol* 2009; **54**: 2167-2173 [PMID: 19942088 DOI: 10.1016/j.jacc.2009.07.042]

19 **Ordovas KG**, Carlsson M, Lease KE, Foster E, Meadows AK, Martin AJ, Hope M, Do L, Higgins CB, Saeed M. Impaired regional left ventricular strain after repair of tetralogy of Fallot. *J Magn Reson Imaging* 2012; **35**: 79-85 [PMID: 22002841 DOI: 10.1002/jmri.22686]

20 **Venkatesh BA**, Schiros CG, Gupta H, Lloyd SG, Dell'Italia L, Denney TS. Three-dimensional plus time biventricular strain from tagged MR images by phase-unwrapped harmonic phase. *J Magn Reson Imaging* 2011; **34**: 799-810 [PMID: 21769965 DOI: 10.1002/jmri.22665]

21 **Khalil M**, Fahmy A, Osman N. Correction of Left Ventricle Strain Signals Estimated from Tagged MR Images. *Int J Future Generation Commun and Net* 2010; **3**: 21

22 **Suffoletto MS**, Dohi K, Cannesson M, Saba S, Gorcsan J. Novel speckle-tracking radial strain from routine black-and-white echocardiographic images to quantify dyssynchrony and predict response to cardiac resynchronization therapy. *Circulation* 2006; **113**: 960-968 [PMID: 16476850 DOI: 10.1161/CIRCULATIONAHA.105.571455]

23 **Lim P**, Buakhamsri A, Popovic ZB, Greenberg NL, Patel D, Thomas JD, Grimm RA. Longitudinal strain delay index by speckle tracking imaging: a new marker of response to cardiac resynchronization therapy. *Circulation* 2008; **118**: 1130-1137 [PMID: 18725491 DOI: 10.1161/CIRCULATIONAHA.107.750190]

24 **Augustine D**, Lewandowski AJ, Lazdam M, Rai A, Francis J, Myerson S, Noble A, Becher H, Neubauer S, Petersen SE, Leeson P. Global and regional left ventricular myocardial deformation measures by magnetic resonance feature tracking in healthy volunteers: comparison with tagging and relevance of gender. *J Cardiovasc Magn Reson* 2013; **15**: 8 [PMID: 23331550 DOI: 10.1186/1532-429X-15-8]

25 **Wu KC**, Zerhouni EA, Judd RM, Lugo-Olivieri CH, Barouch LA, Schulman SP, Blumenthal RS, Lima JA. Prognostic significance of microvascular obstruction by magnetic resonance imaging in patients with acute myocardial infarction. *Circulation* 1998; **97**: 765-772 [PMID: 9498540 DOI: 10.1161/01.CIR.97.8.765]

26 **Galiuto L**. Optimal therapeutic strategies in the setting of post-infarct no reflow: the need for a pathogenetic classification. *Heart* 2004; **90**: 123-125 [PMID: 14729769 DOI: 10.1136/hrt.2003.020800]

27 **Funaro S**, Galiuto L, Boccalini F, Cimino S, Canali E, Evangelio F, DeLuca L, Paraggio L, Mattatelli A, Gnessi L, Agati L. Determinants of microvascular damage recovery after acute myocardial infarction: results from the acute myocardial infarction contrast imaging (AMICI) multi-centre study. *Eur J Echocardiogr* 2011; **12**: 306-312 [PMID: 21367810 DOI: 10.1093/ejechocard/jer009]

28 **Lorenz CH**, Pastorek JS, Bundy JM. Delineation of normal human left ventricular twist throughout systole by tagged cine magnetic resonance imaging. *J Cardiovasc Magn Reson* 2000; **2**: 97-108 [PMID: 11545133 DOI: 10.3109/10976640009148678]

29 **Voigt JU**, Arnold MF, Karlsson M, Hübbert L, Kukulski T, Hatle L, Sutherland GR. Assessment of regional longitudinal myocardial strain rate derived from doppler myocardial imaging indexes in normal and infarcted myocardium. *J Am Soc Echocardiogr* 2000; **13**: 588-598 [PMID: 10849513]

30 **Migrino RQ**, Zhu X, Morker M, Brahmbhatt T, Bright M, Zhao M. Myocardial dysfunction in the periinfarct and remote regions following anterior infarction in rats quantified by 2D radial strain echocardiography: an observational cohort study. *Cardiovasc Ultrasound* 2008; **6**: 17 [PMID: 18445286 DOI: 10.1186/1476-7120-6-17]

31 **Dang AB**, Guccione JM, Mishell JM, Zhang P, Wallace AW, Gorman RC, Gorman JH, Ratcliffe MB. Akinetic myocardial infarcts must contain contracting myocytes: finite-element model study. *Am J Physiol Heart Circ Physiol* 2005; **288**: H1844-H1850 [PMID: 15604126 DOI: 10.1152/ajpheart.00961.2003]

32 **Shin SH**, Hung CL, Uno H, Hassanein AH, Verma A, Bourgoun M, Køber L, Ghali JK, Velazquez EJ, Califf RM, Pfeffer MA, Solomon SD. Mechanical dyssynchrony after myocardial infarction in patients with left ventricular dysfunction, heart failure, or both. *Circulation* 2010; **121**: 1096-1103 [PMID: 20176989 DOI: 10.1161/CIRCULATIONAHA.109.863795]

33 **Mollema SA**, Bleeker GB, Liem SS, Boersma E, van der Hoeven BL, Holman ER, van der Wall EE, Schalij MJ, Bax JJ. Does left ventricular dyssynchrony immediately after acute myocardial infarction result in left ventricular dilatation? *Heart Rhythm* 2007; **4**: 1144-1148 [PMID: 17765611 DOI: 10.1016/j.hrthm.2007.05.018]

34 **Bilchick KC**, Helm RH, Kass DA. Physiology of biven-

tricular pacing. *Curr Cardiol Rep* 2007; **9**: 358-365 [PMID: 17877930]

35   **Cimino S**, Canali E, Petronilli V, Cicogna F, De Luca L, Francone M, Sardella G, Iacoboni C, Agati L. Global and regional longitudinal strain assessed by two-dimensional speckle tracking echocardiography identifies early myocardial dysfunction and transmural extent of myocardial scar in patients with acute ST elevation myocardial infarction and relatively preserved LV function. *Eur Heart J Cardiovasc Imaging* 2013; **14**: 805-811 [PMID: 23258316 DOI: 10.1093/ehjci/jes295]

36   **Charron T**, Jaffe R, Segev A, Bang KW, Qiang B, Sparkes JD, Butany J, Dick AJ, Freedman J, Strauss BH. Effects of distal embolization on the timing of platelet and inflammatory cell activation in interventional coronary no-reflow. *Thromb Res* 2010; **126**: 50-55 [PMID: 20541052 DOI: 10.1016/j.thromres.2010.03.012]

百世登

Baishideng®